Ahvenniemi, Esko; Karppinen, Maarit

In Situ Atomic/Molecular Layer-by-Layer Deposition of Inorganic-Organic Coordination Network Thin Films from Gaseous Precursors

Published in:
Chemistry of Materials

DOI:
10.1021/acs.chemmater.6b02496

Published: 13/09/2016

Document Version
Peer reviewed version

Please cite the original version:
Ahvenniemi, E., & Karppinen, M. (2016). In Situ Atomic/Molecular Layer-by-Layer Deposition of Inorganic-Organic Coordination Network Thin Films from Gaseous Precursors. *Chemistry of Materials*, *28*(17), 6260-6265. https://doi.org/10.1021/acs.chemmater.6b02496

In-situ atomic/molecular layer-by-layer deposition of inorganic-organic coordination network thin films from gaseous precursors

Esko Ahvenniemi and Maarit Karppinen*

Department of Chemistry, Aalto University, P.O. Box 16100, FI-00076 Espoo, Finland

ABSTRACT: Crystalline inorganic-organic coordination network materials possess a property palette highly attractive for a number of frontier applications. In many prospective applications of these materials high-quality thin films would be required. Gas-phase thin-film techniques could potentially provide a number of advantages over the current liquid-phase techniques for depositing such state-of-the-art hybrid thin films. The strongly emerging atomic/molecular layer deposition (ALD/MLD) technique in particular enables the rational fabrication of inorganic-organic thin films in a digital atomic/molecular layer-by-layer manner through successive gas-to-surface reactions of inorganic and organic precursors but the resultant films have been amorphous. Here we demonstrate the in-situ ALD/MLD growth of well-crystalline calcium terephthalate (Ca-TP) coordination network thin films in a wide deposition temperature range. We moreover investigate the water absorption/desorption characteristics of the films and report attractive mechanical properties for both the dry and water-intercalated films.

1. INTRODUCTION

Inorganic-organic coordination network materials have the capacity to combine – in a single-phase material – intrinsic properties of their inorganic and organic constituents, and to show essentially new exciting properties not directly derived from those of the individual building blocks. These materials are moreover relatively stable (both thermally and mechanically) owing to their crystal structures built up of regularly arranged metal cations and large organic linkers. Therefore they are actively investigated for a variety of frontier applications.[1–14] In many prospective applications of these materials high-quality thin films deposited on a specific substrate surface with a precise thickness control and chemisorption-type adhesion would be required. Thin crystalline hybrid films have been deposited using various solution and self-assembled-monolayer methods.[9] However, these techniques might be less suited in producing thin films for applications where strong film-to-substrate adhesion and/or conformality over large-aspect-ratio substrate surfaces are required.[15] Strategies based on gas-phase thin-film deposition techniques, and in particular the state-of-the-art atomic layer deposition (ALD) technique, are believed to potentially meet the aforementioned criteria for film quality and the apparent need for industrial-level scalability.[16] Recently Stassen et al.[17] used a combination of two industrially feasible gas-phase thin-film fabrication techniques, i.e. ALD and CVD (chemical vapor deposition), to – in the first step – deposit crystalline ZnO thin films in an atomic layer-by-layer manner by ALD and then – in the second CVD-type process step – let organic methylimidazole molecules to diffuse from the gas phase into the ZnO matrix to form crystalline ZIF-8 thin films.

The strongly emerging atomic/molecular layer deposition (ALD/MLD) technique where ALD cycles for inorganic constituents are combined with MLD cycles for organic constituents would in principle be an elegant way of fabricating inorganic-organic coordination network thin films;[18–20] it provides us with a simple direct route to build up hybrid metal-organic materials with an atomic/molecular level accuracy for the film thickness and composition even over structurally challenging substrates, as it relies on sequential self-saturated gas-to-surface reactions achieved by pulsing of the precursor materials separately after each time purging the reactor chamber with inert gas. The grand challenge in ALD/MLD has been that the metal-organic hybrid thin films fabricated by the technique have been amorphous even after ordinary post-deposition heat treatments;[18] only a two-step post-deposition annealing treatment under strictly humidity-controlled conditions was shown to yield crystalline coordination network structures.[21] We obtained very recently positive evidence that it is possible to find ALD/MLD fabrication conditions for the in-situ deposition of crystalline metal-organic thin films; our proof-of-the-concept data were for Li-TP and Cu-TP thin films (TP stands for terephthalate).[20,22]

Here we introduce a straightforward and readily reproducible ALD/MLD process for the manufacturing of calcium terephthalate (Ca-TP) coordination network thin films from $Ca(thd)_2$ and benzene-1,4-dicarboxylic acid or so-called terephthalic acid (TPA) precursors over a notably wide deposition temperature range; schematics of our ALD/MLD process are shown in Figure 1. Calcium-terephthalate networks have been synthesized in bulk form and demonstrated to be interesting candidates for example for Li-ion battery anode materials;[23] also known is that the Ca-TP materials synthetized in bulk form tend to have DMF and/or H_2O molecules in their structures, and thus require high-temperature annealing to obtain the solvent-free product.[23–27]

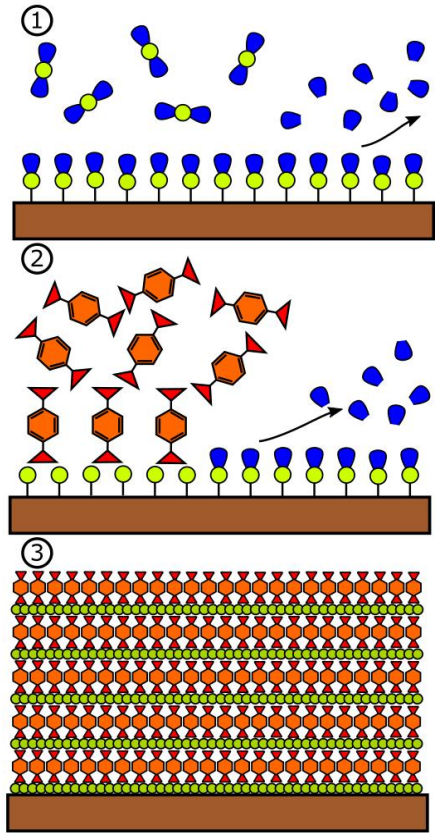

Figure 1. Schematics of the ALD/MLD process for inorganic-organic coordination network thin films, where the process consists of inert-gas-separated pulses of (1) metal (here $Ca(thd)_2$), and (2) organic (here TPA) precursors to yield (3) a monolayer of the hybrid material (here Ca-TP). The film thickness is solely determined by the selected number of repetitions of steps (1) and (2).

2. EXPERIMENTAL SECTION

The Ca-TP thin films were deposited from in-house prepared[28] $Ca(thd)_2$ (thd: 2,2,6,6-tetramethyl-3,5-heptanedione) and commercial terephthalic acid (TPA; 1,4-benzenedicarboxylic acid, Tokyo Chemical Industry CO., Ltd., CAS:100-21-0) precursors. The silicon substrates (625 µm, p-type Si(1 0 0), Okmetic Ltd.) were washed in ethanol/acetone mixture prior deposition, while the polyimide (25 µm, DuPont Kapton CS series) sheets were applied as received. Prior to the deposition, silicon substrates were cut into ca. 25 x 25 mm^2 pieces using a diamond pen, while the polyimide substrates were cut from large sheets into ca. 30 x 30 mm^2 pieces. The films were grown in a commercial hot-wall type ALD reactor of F-120, ASM Microchemistry Ltd. During the depositions, the precursors were kept in glass crucibles inside the reactor, $Ca(thd)_2$ at 190°C and TPA at 180°C.

Structural analyses of the films were performed immediately after the deposition and the samples were stored under vacuum (ca. 15 mbar). After the humidity-treatment tests, the samples were dried in a rapid thermal annealing (RTA) oven (PEO 601 ATV Technologie GmbH) under inert 5.0 Ar gas flow of 200 l/h at 80-100°C for 15 minutes. Grazing incidence X-ray diffraction (GIXRD) and X-ray reflectivity (XRR) measurements were performed using PANalytical model X'Pert PRO diffractometer with Cu K_α radiation. In both measurements, the resolution was 0.05° while the time per step was set to 20 seconds and 6 seconds in GIXRD and XRR, respectively. For the GIXRD measurements, a grazing angle of 0.5° was used. Atomic force microscopy (AFM) experiments were carried out using Veeco Dimension 5000D equipment in tapping mode at 1 Hz frequency. Fourier-transform infrared (FTIR) spectra were collected with Nicolet Magna-IR Spectrometer 750 in transmission mode at 4 cm^{-1} resolution over the 400-4000 cm^{-1} range, and an average of 32 measured spectra was analyzed after the Si substrate spectrum, similarly measured from the same wafer, was subtracted.

Elongation experiments were carried out using a tensile tester of Tensile/Compression Module 5 kN with 100 N load cell, Kammrath & Weiss GmbH where the rate of elongation was 0.5 mm/min. The samples were cut into 2.25 mm wide strips with a custom-made razor blade jig and then glued into abrasive paper, leaving a 10.0 mm long strip available for the tensile test. The samples were measured within a few hours after they were removed from the reactor.

3. RESULTS AND DISCUSSION

In our ALD/MLD process development, we first searched for the optimal temperature range for the depositions by using the following ALD/MLD cycle: 5 s $Ca(thd)_2$ pulse → 2 s N_2 purge → 10 s TPA pulse → 20 s N_2 purge. In Figure 2(a), we plot the growth-per-cycle (GPC) values derived from X-ray reflectivity data, as a function of the deposition temperature. The temperature range investigated was defined by the sublimation temperature of $Ca(thd)_2$ on the lower temperature side and the strongly accelerated desorption of precursors on the higher temperature side. Initially upon increasing the deposition temperature from 185 to 190°C, the growth rate first increases sharply while the opposite is seen for the film density; in this low-temperature range the film quality was also visibly lowered apparently due to a CVD-type growth mode induced by the TPA precursor condensation. Within 190–260°C a plateau is seen for both the growth rate and the film density beyond which the GPC value starts to slowly decline from ca. 3.4 Å/cycle to ca. 0.6 Å/cycle at 420°C. Since the XRR-derived film density stays nearly constant (1.7-1.8 g/cm^3) for the entire deposition temperature range of 190–420°C, this suggests the reason for the declining growth rate to arise from an increasing precursor desorption rate when the deposition temperature is increased, while the film quality seems to remain the same.

Next we investigated the required precursor pulsing lengths; for these experiments shown in Figure 2(b,c) the deposition temperature was fixed at 220°C and the initial choice for the pulse/purge lengths was, 5 s $Ca(thd)_2$ pulse → 2 s N_2 purge → 10 s TPA pulse → 20 s N_2 purge, which was then refined by changing one parameter at a time to end up with the following optimized deposition parameters for the rest of the experiments: 5 s $Ca(thd)_2$ → 5 s N_2 purge → 10 s TPA pulse → 15 s N_2 purge. As seen in Figure 2(d), the thus deposited films grow in a highly linear (R^2 = 0.9983) manner in the entire thickness range of 15–180 nm investigated; the surface roughness increases nearly linearly (R^2 = 0.910) with increasing film thickness, as commonly seen for crystalline films. We moreover confirmed these XRR-based film roughness values by AFM for one sample (52.8 nm thick; deposited at 220°C and stored in vacuum prior to the measurement): the RMS roughness

value calculated at 1.88 nm perfectly agrees with the XRR-derived value. From AFM, the films constitute of evenly distributed crystallites of ca. 50 x 100 nm^2 in size.

The GIXRD patterns collected for the films (Figure 3) verify that all our Ca-TP films are crystalline independent of the deposition temperature used (190–420°C). Moreover, the crystal structure of the as-deposited films is essentially compatible with the "dry" Ca-TP structure previously reported for bulk samples;[27] it is a rather common feature that GIXRD data somewhat differ from the corresponding XRD data in terms of the peak intensities and even slightly for the peak positions due to e.g. residual stress.[29,30] Here the slight shift of the peak positions to the lower 2θ values could also indicate the beginning of the H2O absorption. When the films were stored under notably humid conditions they absorbed water into the crystal structure such that the structure transformed to a structure similar to that reported for bulk samples of "trihydrated" Ca-TP.[31] The two crystal structures, i.e. both the dry and trihydrated structure forms, are composed of 3-dimensional coordination networks, where the calcium atoms are coordinated to the organic molecules via oxygen atoms, see Figure 3. It should also be mentioned that our XRR-derived density values of 1.7-1.8 g/cm^3 for both the structures agree reasonably well with the densities calculated for the dry and trihydrated phases from the reported unit cell parameters, i.e. 2.03 and 1.71 g/cm^3, respectively. The change from the dry to the trihydrated phase did not result in any notable change in the roughness value.

To further examine the calcium-to-carboxylate bonds and to confirm the absence of impurities, FTIR spectra were measured for representative as-deposited samples of the dry Ca-TP structure and air-exposed samples of the trihydrated structure, see Figure 3. From FTIR spectra for the dry samples, the absence of features in the 1700–3500 cm^{-1} range due to coordinated H_2O, COOH or hydrocarbons is evident, as expected. We may thus conclude that during the ALD/MLD process the carboxylic acid precursor completely reacts to form the carboxylate-calcium bond and that the ligands of $Ca(thd)_2$ are completely dispatched during the deposition process. The signature area of 1250–1650 cm^{-1} in the FTIR spectra holds most of the interesting vibrations.[31] Benzene ring peaks can be seen at 1625 cm^{-1} (aromatic C=C), 1435 cm^{-1} (ring structure) and 1505 cm^{-1} (aromatic C=C), the C-O peak at 1310 cm^{-1} and the COO-peaks at 1580 cm^{-1} (asymmetric) and 1395 cm^{-1} (symmetric). The type of the carboxylate-calcium bond can be either bridging, unidentate or bidentate, and it can be evaluated from the splitting between the symmetric (v_s) and asymmetric (v_{as}) stretches of the COO^- group, typically seen in the 1650–1250 cm^{-1} area.[32] Indeed, the $\Delta(v_{as}-v_s)$ value in the present case is ca. 185 cm^{-1}, which implies bridging-type coordination, in line with the expected dry crystal structure shown in Figure 3. For the humid-air-exposed films of the trihydrated structure FTIR patterns reveal the characteristic sharp peaks of coordinated water molecules at ca. 3512, 3470 and 3305 cm^{-1}. The asymmetric and symmetric stretches of the carboxylate group are seen at 1555 and 1390 cm^{-1}, respectively, the resultant splitting value of $\Delta(v_{as}-v_s)$ = 165 cm^{-1} suggesting a bridging-type coordination in this case as well. Benzene ring stretching features are similarly seen at 1620 (w), 1510 cm^{-1} (s) and 1435 cm^{-1} (s). The absence of any band between 1680 and 1800 cm^{-1} reveals that only deprotonated carboxylic groups are present in the film.[27]

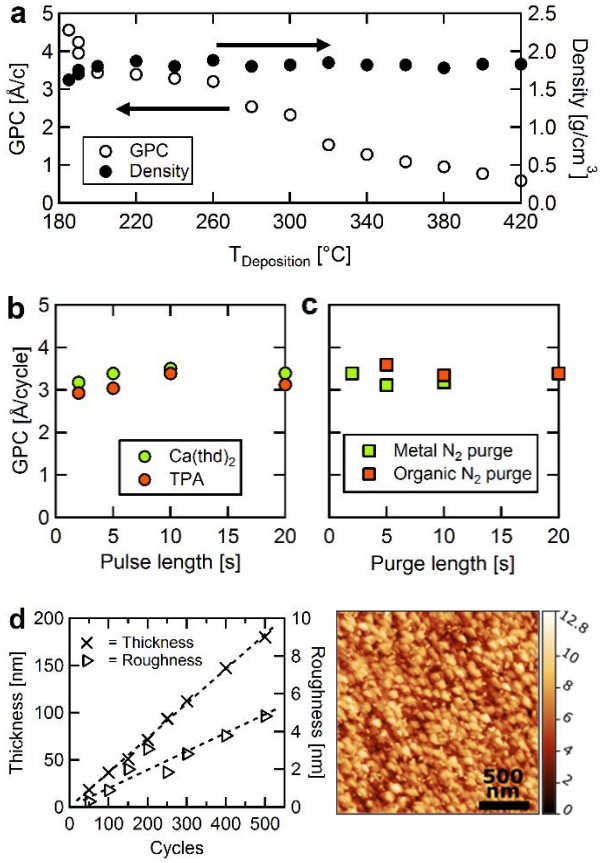

Figure 2. Deposition characteristics to demonstrate the controllability of the ALD/MLD process for our Ca-TP thin films: (a) Homogeneous films are obtained in a well-controlled manner and with a high growth rate in the appreciably wide temperature range of 200–420°C. The GPC value (data from depositions at 220°C) saturates already for short (b) precursor and (c) purge lengths, and (d) the film thickness increases linearly with the number of ALD/MLD cycles; all these characteristics manifest an ideal ALD/MLD process. (d) Both XRR and AFM data show that the surface roughness increases with increasing film thickness as expected for in-situ crystallized films.

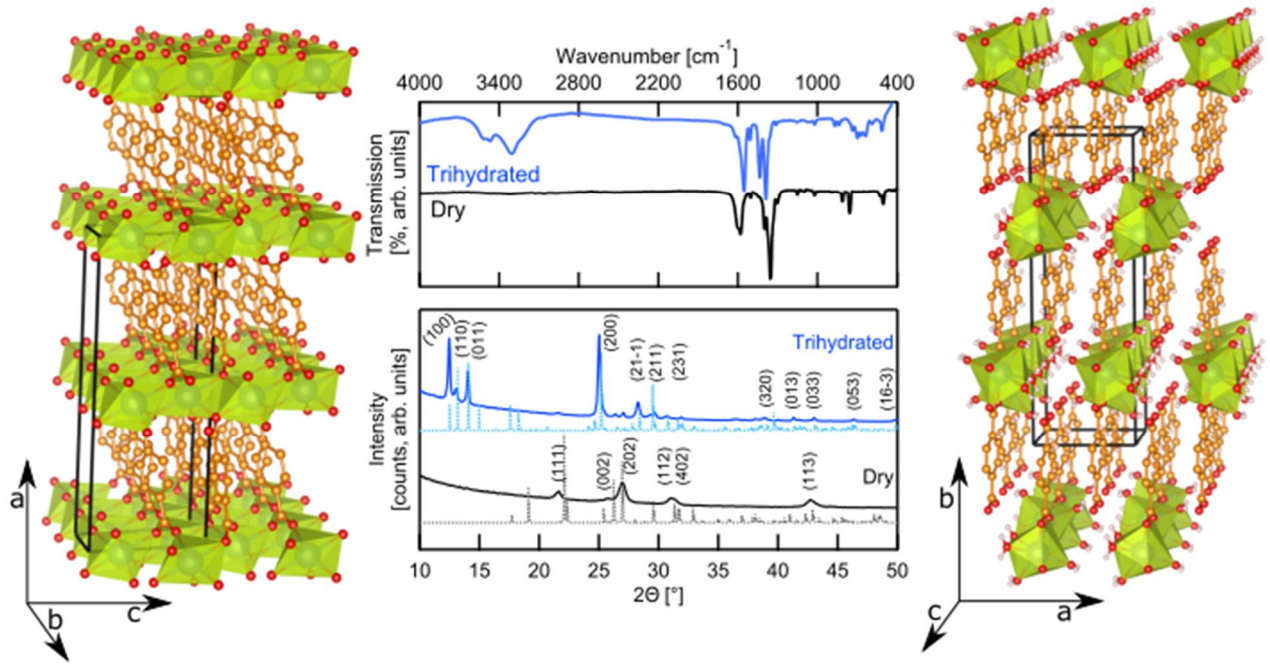

Figure 3. Left and right: dry (space group C2/c)[27] and trihydrated (space group $P2_1/c$)[31] Ca-TP structures viewed along the layer-piling direction; structures drawn using Fullprof and VESTA softwares. Both the FTIR spectra (top graphs) and GIXRD patterns (bottom graphs) collected for the Ca-TP films are essentially compatible with the crystal structures reported for bulk samples; the fainter XRD patterns below the experimental GIXRD patterns are calculated based on the reported bulk crystal structures, and for our thin films of the dry and trihydrated structures the lattice parameters were refined as follows, respectively: a = 18.6 Å, b = 5.19 Å, c = 6.93 Å, β = 86.7°, and a = 7.07 Å, b = 21.6 Å, c = 6.58 Å, β = 92.6°.

We moreover investigated representative samples of both dry and trihydrated Ca-TP films for their mechanical properties using a tensile tester. In the top part of Figure 4, the assumed outcome of the elongation experiments is illustrated, where in panel (1) only the substrate's elongation profile is initially seen. In panel (2), the breaking of the thin film is seen as a small dent in the force-to-elongation curve and finally, in panel (3) the breaking of the substrate is seen as a sharp and complete drop of the signal. To perform the elongation experiments, a 420-nm thick Ca-TP film was deposited on a 25-µm thick polyimide film. First we elongated several plain polyimide strips to determine the base elongation profile of the substrate; several parallel experiments revealed the breakage point for the substrate at 33 % in average. In Figure 4 (bottom plots), the actual elongation measurement data for our thin-film samples are displayed. The trihydrated (humid-air-exposed) Ca-TP films were found to tolerate elongations on average ca. 23 % before breaking (calculated from five parallel experiments), while the dry Ca-TP films from the same sample batch were found to break already at ca. 1.5–2.0 % elongation. Nevertheless, even the dry Ca-TP films show relatively good resiliency towards induced tensile stress. It was expected that the two different crystal structures would perform in a slightly different manner, but such a significance difference in the performance was found somewhat exciting. We tentatively ascribe the superior performance of the trihydrated Ca-TP film to the fact that the films were elongated along the Ca-atom planes and while the dry structure may not have much room for expansion before the film is broken, the trihydrated structure has massive amounts of non-bound COO^- groups aligned in a zipper-like structure to give room for expansion without damaging the actual structure. Excellent elastic properties have been predicted from calculation for various hybrid coordination network structures;[10,33] however as far as the authors know only compressibility and shear modulus but not elasticity have been experimentally studied.

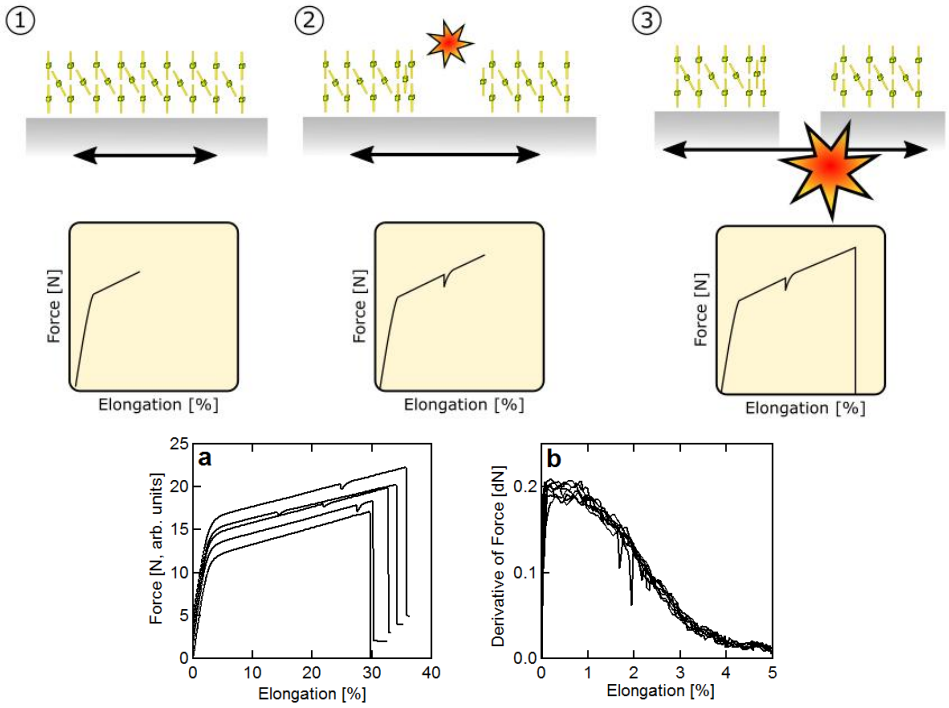

Figure 4. Elongation test results for 420 nm thick Ca-TP films on a polyimide substrate. The illustration panels on top and middle describe the expected force-to-elongation graphs for thin-film + thick-substrate systems: in panel (1) only the substrate's elongation profile is initially seen, then the breakage of the thin film is seen as a small but sharp drop in panel (2) before the breakage of the substrate later on in panel (3). Bottom graphs show experimental elongation curves for representative Ca-TP thin film samples; the thin-film breakage is visible in the force curves (a) for the trihydrated films and in the derivative curves (b) for the dry films.

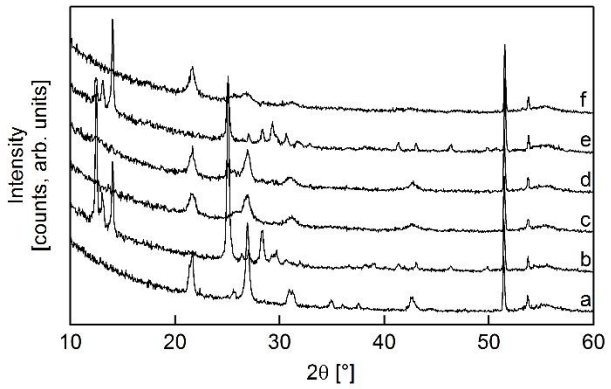

Figure 5. GIXRD patterns taken for a representative Ca-TP thin-film sample after first (a) exposing it to open air for less than 15 minutes, then (b) keeping it in 30% RH air at 25°C for 90 days, (c) regenerating it in Ar gas flow at 100°C for 15 minutes, (d) keeping it in 30% RH air at 25°C for 24 hours, (e) force-wetting it under 50°C Millipore water vapor for 4 hours, and finally (f) regenerating it in Ar gas flow at 80°C for 15 minutes. In (a), (c), (d) and (f) the sample is in an essentially phase-pure form of the dry phase, and in (b) and (e) of the trihydrated phase.

Finally a series of tests were conducted to investigate the reversibility plus the speed and the readiness of the water absorption/desorption processes of our Ca-TP thin films. A representative as-deposited dry sample was in turns exposed to humidity at room temperature, then dried in an RTA oven in Ar gas flow at 80-100°C for 15 minutes. From the resultant GIXRD patterns displayed in Figure 5 it is seen that the phase change is indeed completely reversible even at the low regeneration temperature. It is interesting to note that for the thin films the regeneration temperature seems to be much lower in comparison with bulk Ca-TP for which a previous study estimated the plausible regeneration temperature around 400°C from thermogravimetric data.[27]

4. CONCLUSIONS

We demonstrated in this work that crystalline inorganic-organic coordination network thin films can be fabricated in a single-step process from gaseous precursors within a notably wide deposition temperature window of at least 190~420 °C. Most importantly, the industrially-feasible ALD/MLD technique employed for the depositions allows the growth of these materials with atomic/molecular layer thickness precision on various (sensitive, flexible, complex, *etc.*) substrate surfaces. We carried out preliminary tests to demonstrate that our ALD/MLD grown hybrid thin films absorb and release water molecules reversibly and in particular that they can be regenerated at appreciably low temperatures. Moreover shown was that the films possess highly promising mechanical properties.

Our results here were for Ca-TP thin films but we foresee that our ALD/MLD approach has the capacity to be extended beyond the Ca-TP thin films to cover other exciting hybrid coordination network materials as well that need to be deposited as high-quality (in terms of adhesion, homogeneity, conformity, etc.) thin films over e.g. delicate or complex surfaces. Such thin-film hybrid materials are desired for the next-generation application in e.g. electronics, sensors, sieves and other high-technology products.

AUTHOR INFORMATION

Corresponding Author

* E-mail: maarit.karppinen@aalto.fi

Notes

The authors declare no competing financial interest.

Author Contributions

The manuscript was written through contributions of all authors

ACKNOWLEDGMENTS

The present work has received funding from the European Research Council under the European Union's Seventh Framework Programme (FP/2007-2014)/ERC Advanced Grant Agreement (no. 339478). We thank Mr. Mikko Nisula for assistance in Fullprof analysis and Mr. Mikko Toivonen for assistance in mechanical characterizations, and Nanotalo premises for the use of tensile testing and AFM equipment.

REFERENCES

(1) Bétard, A.; Fischer, R. A. Metal-Organic Framework Thin Films: From Fundamentals to Applications, *Chem. Rev.* 2012, 112, 1055–1083.

(2) Yaghi, O. M.; O'Keeffe, M.; Ockwig, N. W.; Chae, H. K.; Eddaoudi, M.; Kim, J. Reticular synthesis and the design of new materials, *Nature* 2003, *423*, 705–714.

(3) Furukawa, H.; Cordova, K. E.; O'Keeffe, M.; Yaghi, O. M. The Chemistry and Applications of Metal-Organic Frameworks, *Science* 2013, 341, 1230444.

(4) Horcajada, P.; Serre, C.; Maurin, G.; Ramsahye, N. A.; Balas, F.; Vallet-Regí, M.; Sebban, M.; Taulelle, F.; Férey, G. Flexible Porous Metal-Organic Frameworks for a Controlled Drug Delivery, *J. Am. Chem. Soc.* 2008, 130, 6774–6780.

(5) Lee, J.; Farha, O. K.; Roberts, J.; Scheidt, K. A.; Nguyen, S. T.; Hupp, J. T. Metal-Organic Framework Materials as Catalysts, *Chem. Soc. Rev.* 2009, 38, 1450–1459.

(6) Li, W.; Probert, M. R.; Kosa, M.; Bennett, T. D.; Thirumurugan, A.; Burwood, R. P.; Parrinello, M.; Howard, J. A. K.; Cheetham, A. K. Negative Linear Compressibility of a Metal-Organic Framework, *J. Am. Chem. Soc.* 2012, 134, 11940–11943.

(7) Kühne, D.; Klappenberger, F.; Decker, R.; Schlickum, U.; Brune, H.; Klyatskaya, S.; Ruben, M.; Barth, J. V. High-Quality 2-D Metal-Organic Coordination Network Providing Giant Cavities within Mesoscale Domains, *J. Am. Chem. Soc.* 2009, *131*, 3881–3883.

(8) Ke, F.-S.; Wu, Y.-S.; Deng, H. Metal-Organic Frameworks for Lithium Ion Batteries and Supercapacitors, *J. Solid State Chem.* 2015, 223, 109–121.

(9) Shekhah, O.; Liu, J.; Fischer, R. A.; Wöll, C. MOF Thin Films: Existing and Future Applications, *Chem. Soc. Rev.* 2011, 40, 1081–1106.

(10) Horike, S.; Shimomura, S.; Kitagawa, S. Soft Porous Crystals, *Nat. Chem.* 2009, 1, 695–704.

(11) Ameloot, R.; Vermoortele, F.; Vanhove, W.; Roeffaers, M. B. J.; Sels, B. F.; De Vos, D. E. Interfacial Synthesis of Hollow-Metal-Organic Framework Capsules Demonstrating Selective Permeability, *Nat. Chem.* 2011, 3, 382–387.

(12) Férey, G.; Mellot-Draznieks, C.; Serre, C.; Millange, F. Crystallized Frameworks with Giant Pores: Are There Limits to the Possible?, *Acc. Chem. Res.* 2005, 38, 217–225.

(13) Carson, C. G.; Brunnello, G.; Lee, S. G.; Jang, S. S.; Gerhardt, R. A.; Tannenbaum, R. Structure Solution from Powder Diffraction of Copper 1,4-benzenedicarboxylate, *Eur. J. Inorg. Chem.* 2014, 2140–2145.

(14) Forster, P. M.; Eckert, J.; Heiken, B. D.; Parise, J. B.; Yoon, J. W.; Jhung, S. H.; Chang, J.-S.; Cheetham, A. K. Adsorption of Molecular Hydrogen on Coordinatively Unsaturated Ni(II) Sites in a Nanoporous Hybrid Material, *J. Am. Chem. Soc.* 2006, 128, 16846–16850.

(15) Bradshaw, D.; Garai, A.; Huo, J. Metal-Organic Framework Growth at Functional Interfaces: Thin Films and Composites for Diverse Applications, *Chem. Soc. Rev.* 2012, 41, 2344–2381.

(16) Allendorf, M. D.; Stavila, V. From Conventional to Conformal, *Nat. Mater.* 2016, 15, 255–257.

(17) Stassen, I.; Styles, M.; Grenci, G.; Gorp, H. Van;

Vanderlinden, W.; Feyter, S. De; Falcaro, P.; Vos, D. De; Vereecken, P.; Ameloot, R. Chemical Vapour Deposition of Zeolitic Imidazolate Framework Thin Films, *Nat. Mater.* 2015, 15, 304–310.

(18) Sundberg, P.; Karppinen, M. Organic and Inorganic-Organic Thin Film Structures by Molecular Layer Deposition: A Review, *Beilstein J. Nanotechnol.* 2014, 5, 1104–1136.

(19) George, S. M. Atomic Layer Deposition: An Overview, *Chem. Rev.* 2010, 110, 111–131.

(20) Ahvenniemi, E.; Karppinen, M. Atomic/Molecular Layer Deposition: A Direct Gas-phase Route to Crystalline Metal-Organic Framework Thin Films, *Chem. Commun.* 2016, 52, 1139–1142.

(21) Salmi, L. D.; Heikkilä, M. J.; Puukilainen, E.; Ritala, M.; Sajavaara, T. Studies on atomic layer deposition of IRMOF-8 thin films, *J. Vac. Sci. Technol. A* 2015, *33*, 01A121.

(22) Nisula, M.; Karppinen, M. Atomic/Molecular Layer Deposition of Lithium Terephthalate Thin Films as High Rate Capability Li-ion Battery Anodes, *ACS Nano Lett.* 2016, 16, 1276–1281.

(23) Wang, L.; Mou, C.; Sun, Y.; Liu, W.; Deng, Q.; Li, J. Structure-Property of Metal Organic Frameworks Calcium Terephthalates Anodes for Lithium-ion Batteries, *Electrochim. Acta* 2015, 173, 235–241.

(24) Zhang, X.; Huang, Y. Y.; Zhang, M. J.; Zhang, J.; Yao, Y. G. A Series of Ca(II) or Ba(II) Inorganic-Organic Hybrid Frameworks Based on Aromatic Polycarboxylate Ligands with the Inorganic M-O-M (M = Ca, Ba) Connectivity from 1D to 3D, *Cryst. Growth Des.* 2012, 12, 3231–3238.

(25) Liang, P.-C.; Liu, H.-K.; Yeh, C.-T.; Lin, C.-H.; Zima, V. Supramolecular Assembly of Calcium Metal-Organic Frameworks with Structural Transformations, *Cryst. Growth Des.* 2011, 11, 699–708.

(26) Panasyuk, G. P.; Azarova, L. A.; Khaddaj, M.; Budova, G. P.; Voroshilov, I. L.; Grusha, T. V.; Izotov, A. D. Preparation and Properties of Sodium, Potassium, Magnesium, Calcium, and Aluminum Terephthalates, *Inorg. Mater.* 2003, 39, 1292–1297.

(27) Mazaj, M.; Mali, G.; Rangus, M.; Žunkovič, E.; Kaučič, V.; Logar, N. Z. Spectroscopic Studies of Structural Dynamics Induced by Heating and Hydration: A Case of Calcium-Terephthalate Metal-Organic Frameworks, *J. Phys. Chem. C* 2013, 117, 7552–7564.

(28) Hammond, G. S.; Nonhebel, D. C.; Wu, C.-H. S. Chelates of β-Diketonates. V. Preparation and Properties of Chelates Containing Sterically Hindered Ligands, *Inorg. Chem.* 1963, 2, 73–76.

(29) Neerinck, D. G.; Vink, T. J. Depth Profiling of Thin ITO films by Grazing Incidence X-Ray Diffraction, *Thin Solid Films* 1996, 278, 12–17.

(30) Gelfi, M.; Bontempi, E.; Roberti, R.; Armelao, L.; Depero, L. E. Residual Stress Analysis of Thin Films and Coatings Through XRD^2 Experiments, *Thin Solid Films* 2004, 450, 143–147.

(31) Dale, S. H.; Elsegood, M. R. J. *catena*-Poly[[diaquacalcium(II)]-μ_3-terephthalato-μ_2-aqua] at 150 K, Acta *Crystallogr. Sect. E* 2003, 59, m586–m587.

(32) Klepper, K. B.; Nilsen, O.; Francis, S.; Fjellvåg, H. Guidance of Growth Mode and Structural Character in Organic-Inorganic Hybrid Materials - A Comparative Study, *Dalton Trans.* 2014, 43, 3492.

(33) Ortiz, A. U.; Boutin, A.; Fuchs, A. H.; Coudert, F. X. Anisotropic Elastic Properties of Flexible Metal-Organic Frameworks: How Soft Are Soft Porous Crystals?, *Phys. Rev. Lett.* 2012, 109, 1–5.

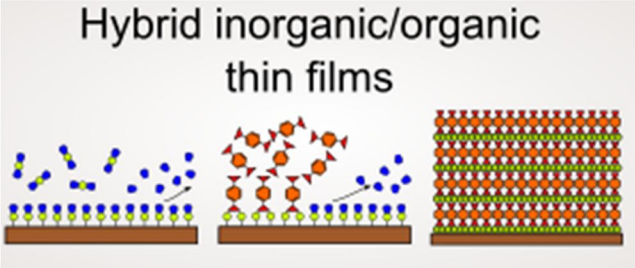

For table of contents only